Single Photon Source and Photon Statistics

Objectives:

- In this laboratory experiment students will familiarize with a micro-photoluminescence optical setup and the necessary optical devices for the detection and counting of photons.
- Students will observe the quantum nature of light and understand the underlying principle behind photon counting and fluctuations.
- Students will verify photon statistics for the demonstration of single-photon sources, coherent light and chaotic light sources.
- Students will also familiarize with sample preparation techniques for single-molecule spectroscopy.

1. Introduction

When considering a beam of light as a stream of photons rather than as a classical wave, it turns out that the differences are rather subtle. One has to look quite hard to see significant departures from the predictions of the classical theories. In this experiment we will approach the subject from the perspective of the statistical properties of the photon stream. In the following, the principle behind photon counting will be presented and further detail can be found in reference [1].

The detection of a light beam by a photon counter as illustrated in Figure 1. The photon counter consists of a very sensitive light detector such as an avalanche photodiode (APD) or photomultiplier tube (PMT) connected to an electronic counter. The detector produces short voltage pulses in response to the light beam and the counter registers the number of pulses that are emitted within a certain time interval set by the user. Photon counters thus operate in a very similar way to the Geiger counters used to count the particles emitted by the decay of radioactive nuclei.

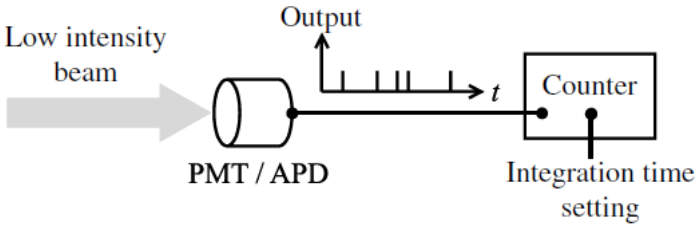

Figure 1. Detection of a faint light beam by a PMT or APD and pulse counting electronics.

The detector emits individual pulses for the impinging light beam that consists of a stream of discrete energy packets that we generally call ‘photons’. The fluctuations in the count rate would give information about the statistical properties of the incoming photon stream.

In this kind of experiments one has to distinguish carefully between:

(1) the statistical nature of the photo-detection process;
(2) the intrinsic photon statistics of the light beam.

1.1 . Photon-counting statistics

Here we want to answer two fundamental questions 1) Why does the number of photons fluctuate on short time-scales? 2) Is the fluctuation intrinsic or due to experimental problems?

Let us consider the outcome of a photon-counting experiment as illustrated in Figure 1. The basic idea is to count the number of photons that strike the detector in a user-specified time interval *T*. We start with the simplest case and consider the detection of a perfectly coherent monochromatic beam of angular frequency ω and constant intensity *I*. In the quantum picture of light, the beam consists of a stream of photons. The photon flux Φ is defined as the average number of photons passing through a cross-section of the beam in unit time. Φ is easily calculated by dividing the energy flux by the energy of the individual photons:

$$\Phi = \frac{IA}{\hbar\omega} \equiv \frac{P}{\hbar\omega} \text{ photons s}^{-1},$$

where *A* is the area of the beam and *P* is the power.

Photon-counting detectors are specified by their quantum efficiency η, which is defined as the ratio of the number of photocounts to the number of incident photons. The average number of counts registered by the detector in a counting time *T* is thus given by:

$$N(T) = \eta\Phi T = \frac{\eta PT}{\hbar\omega}.$$

The corresponding average count rate *R* is given by:

$$\mathcal{R} = \frac{N}{T} = \eta\Phi = \frac{\eta P}{\hbar\omega} \text{ counts s}^{-1}.$$

The maximum count rate that can be registered with a photon-counting system is usually determined by the fact that the detectors need a certain amount of time to recover after each detection event, which means that a 'dead time' of ~ *70* ns - 1 μs must typically elapse between successive counts. This sets a practical upper limit on *R* of around 10^6 counts s^{-1}. With typical values of η for modern detectors of 30-70 % or more, the above equation shows that photon counters are only useful for analysing the properties of very faint light beams with optical powers of $\sim 10^{-12}$ W or less. The detection of light beams with higher power levels is done by a different method.

The photon flux and the detector count rate equations given above represent the *average* properties of the beam. A beam of light with a well-defined average photon flux will nevertheless show photon number fluctuations at short time intervals. This is a consequence of the inherent 'graininess' of the beam caused by chopping it up into photons. We can see this more clearly with the aid of a simple example. Consider a beam of light of photon energy 2.0 eV with an average power of 1 nW. Such a beam could be obtained by taking a He-Ne laser operating at 633 nm with a power of 1 mW and attenuating it by a factor 10^6 by using neutral density filters. The average photon flux is:

$$\Phi = \frac{10^{-9}}{2.0 \times (1.6 \times 10^{-19})} = 3.1 \times 10^9 \text{ photons s}^{-1}.$$

Since the velocity of light is 3×10^8 m/s, a segment of the beam with a length of 3×10^8 m would contain 3.1×10^9 photons on average. On a smaller scale, we would expect an average of 31 photons within a 3 m segment of beam. In still smaller segments, the average photon number becomes fractional. For example, a 1-ns count time corresponds to a 30 cm segment of beam, and contains an average of 3.1 photons. Now photons are discrete energy packets, and the actual number of photons has to be an integer. We must therefore have an integer number of photons in each beam segment, as illustrated in Figure 2. In the next section we shall show that if we assume that the photons are equally likely to be at any point within the beam, then we find random fluctuations above and below the mean value. If we were to look at 30 such beam segments, we might therefore find a sequence of photon counts that looks something like:
1, 6, 3, 1, 2, 2, 4, 4, 2, 3, 4, 3, 1, 3, 6, 5, 0, 4, 1, 1, 6, 2, 2, 6, 4, 1, 4, 3, 4, 6. Statistical analysis of this sequence, which is based on uniform random numbers, gives a sum of 95, a mean of 3.16, and a standard deviation of 1.81. The statistical fluctuations arise from the fact that we do not know exactly where the photons are within the beam.

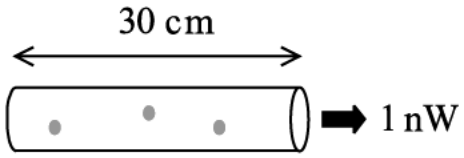

Figure 2. A 30 cm section of a beam light at 633 nm with a power of 1 nW contains three photons on average.

If we make the length of the segments even smaller, the fluctuations become even more apparent. For example, in a 3 cm segment of beam corresponding to a time interval of 100 ps, the average photon number falls to 0.31. The majority of beam segments are now empty, and a sequence of 10 beam segments equivalent to any one of the 30 cm segments considered above might look like: 1, 0, 0, 1, 0, 0, 0, 0, 0, 1. This sequence has a sum of 3, a mean of 0.3, and a standard deviation of 0.46. It is apparent that the shorter the time interval, the more difficult it becomes to know where the photons are. Thus if we split the 30 cm beam segment shown in Figure 2 into 1000 intervals of 0.3 mm length and 1 ps duration, we would find that typically only three intervals contain photons, and 997 are empty. We have no way of predicting which three of these 1000 segments contain the photons. These examples show that although the average photon flux can have a well-defined value, the photon number on short time-scales fluctuates due to the discrete nature of the photons. These fluctuations are described by the photon statistics of the light. In the following sections, we shall investigate the statistical nature of various types of light, starting with the simplest case, namely a perfectly stable monochromatic light source.

1.2 . Coherent light: Poissonian photon statistics

In classical physics, light is considered to be an electromagnetic wave. The most stable type of light that we can imagine is a perfectly coherent light beam which has constant angular frequency ω, phase φ, and amplitude E_0:

$$\mathcal{E}(x,t) = \mathcal{E}_0 \sin(kx - \omega t + \phi),$$

where $E(x, t)$ is the electric field of the light wave and $k = \omega/c$ in free space. The beam emitted by an ideal single-mode laser operating well above threshold is a reasonably good approximation to such a field. The intensity I of the beam is proportional to the square of the amplitude, and is constant if E_0 and φ are independent of time. There will therefore be no intensity fluctuations and the average photon flux defined earlier will be constant in time.

It might be thought that a beam of light with a time-invariant average photon flux would consist of a stream of photons with regular time intervals between them. This is not in fact the case. We have seen above that there must be statistical fluctuations on short time-scales due to the discrete nature of the photons. We shall now show that perfectly coherent light with a constant intensity has Poissonian photon statistics.

Consider a light beam of constant power P. The average number of photons within a beam segment of length L is given by

$$\overline{n} = \Phi L/c,$$

where Φ is the photon flux. We assume that L is large enough that $\overline{n}$ takes a well-defined integer value. We now subdivide the beam segment into N subsegments of length L/N. N is assumed to be sufficiently large that there is only a very small probability $p = \overline{n}/N$ of finding a photon within any particular subsegment, and a negligibly small probability of finding two or more photons.

We now ask: what is the probability $P(n)$ of finding n photons within a beam of length L containing N subsegments? The answer is given by the probability of finding n subsegments containing one photon and $(N - n)$ containing no photons, in any possible order. This probability is given by the binomial distribution:

$$\mathcal{P}(n) = \frac{N!}{n!(N-n)!}\, p^n\, (1-p)^{N-n},$$

which, with $p = \overline{n}/N$, gives

$$\mathcal{P}(n) = \frac{N!}{n!(N-n)!}\, \left(\frac{\overline{n}}{N}\right)^n\, \left(1 - \frac{\overline{n}}{N}\right)^{N-n}.$$

We now take the limit as $N \to \infty$. To do this, we first rearrange the above equation in the following form:

$$\mathcal{P}(n) = \frac{1}{n!}\, \left(\frac{N!}{(N-n)!N^n}\right)\, \overline{n}^n\, \left(1 - \frac{\overline{n}}{N}\right)^{N-n}.$$

Now by using Stirling's formula:

$$\lim_{N\to\infty}[\ln N!] = N\ln N - N,$$

we can see that

$$\lim_{N\to\infty}\left[\ln\left(\frac{N!}{(N-n)!N^n}\right)\right] = 0.$$

Hence:

$$\lim_{N\to\infty}\left[\frac{N!}{(N-n)!N^n}\right] = 1.$$

Furthermore, by applying the binomial theorem and comparing the result for the limit $N \to \infty$ to the series expansion of $\exp(-n)$, we can see that:

$$\begin{aligned}\left(1-\frac{\overline{n}}{N}\right)^{N-n} &= 1-(N-n)\frac{\overline{n}}{N}+\frac{1}{2!}(N-n)(N-n-1)\left(\frac{\overline{n}}{N}\right)^2-\cdots\\ &\to 1-\overline{n}+\frac{\overline{n}^2}{2!}-\cdots\\ &= \exp(-\overline{n}).\end{aligned}$$

On using these two limits, we find

$$\lim_{N\to\infty}[\mathcal{P}(n)] = \frac{1}{n!}\cdot 1\cdot\overline{n}^n\cdot\exp(-\overline{n}).$$

We thus conclude that the photon statistics for a coherent light wave with constant intensity are given by:

$$\mathcal{P}(n) = \frac{\overline{n}^n}{n!}\mathrm{e}^{-\overline{n}}, \quad n = 0,\ 1,\ 2,\ \cdots.$$

This equation describes a Poisson distribution. Poissonian statistics generally apply to random processes that can only return integer values.

Poisson distributions are uniquely characterized by their mean value $\overline{n}$. Representative distributions for $\overline{n}$ =0.1, 1, 5, and 10 are shown in Figure 3. It is apparent that the distribution peaks at $\overline{n}$ and gets broader as $\overline{n}$ increases. The fluctuations of a statistical distribution about its mean value are usually quantified in terms of the variance. The variance is equal to the square of the standard deviation Δn and is defined by:

$$\mathrm{Var}(n) \equiv (\Delta n)^2 = \sum_{n=0}^{\infty}(n-\overline{n})^2\mathcal{P}(n).$$

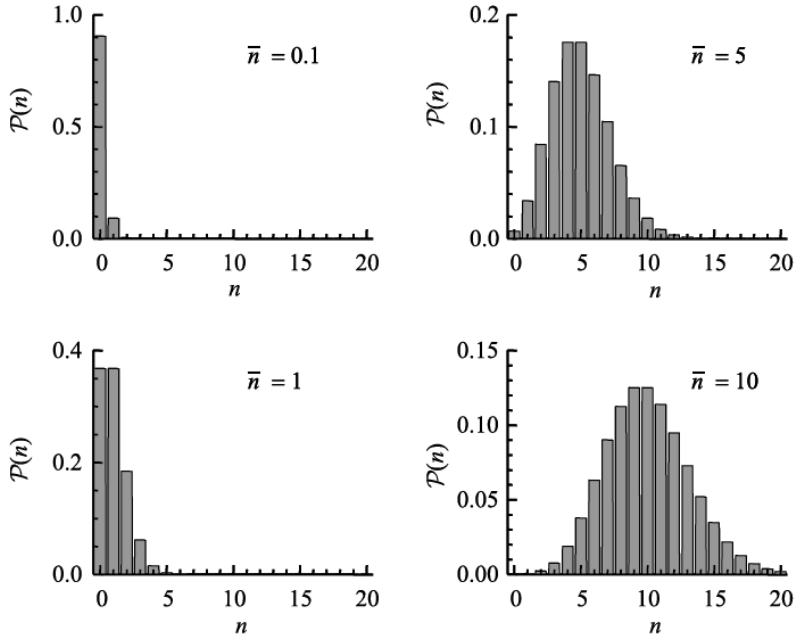

Figure 3. Poisson distributions for mean values of 0.1, 1, 5, and 10. Note that the vertical axis scale changes between each figure.

It is a well-known result for Poisson statistics that the variance is equal to the mean value $\bar{n}$

$$(\Delta n)^2 = \bar{n}.$$

The standard deviation for the fluctuations of the photon number above and below the mean value is therefore given by:

$$\Delta n = \sqrt{\bar{n}}.$$

This shows that the relative size of the fluctuations decreases as $\bar{n}$ gets larger. If $\bar{n}$ =1, we have Δn = 1 so that $\Delta n/\bar{n}$ =1. On the other hand, if $\bar{n}$ =100, we have Δn =10, and $\Delta n/\bar{n}$ =0.1.

1.3 . Classification of light by Photon statistics

In the previous section, we considered the photon statistics of a perfectly coherent light beam with constant optical power *P*. From a classical perspective, a perfectly coherent beam of constant intensity is the most stable type of light that can be envisaged. This therefore provides a bench mark for classifying other types of light according to the standard deviation of their photon number distributions. In general, there are three possibilities:

- sub-Poissonian statistics: $\Delta n < \sqrt{\bar{n}}$
- Poissonian statistics: $\Delta n = \sqrt{\bar{n}}$
- super-Poissonian statistics: $\Delta n > \sqrt{\bar{n}}$

The difference between the three different types of statistics is illustrated in Figure 4. This figure compares the photon number distributions of super-Poissonian and sub-Poissonian light to that

of a Poisson distribution with the same mean photon number. We see that distributions of super-Poissonian and sub-Poissonian light are, respectively, broader or narrower than the Poisson distribution.

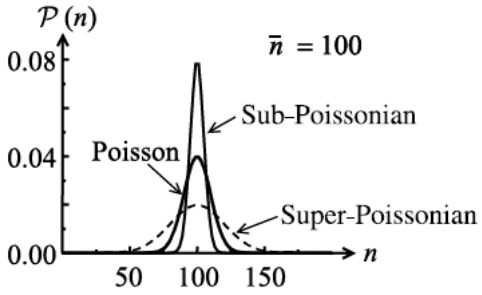

Figure 4. Comparison of the photon statistics for light with a Poisson distribution, and those for sub-Poissonian and super-Poissonian light. The distributions have been drawn with the same mean photon number $\bar{n}$ = 100. The discrete nature of the distributions is not apparent in this figure due to the large value of $\bar{n}$.

It is not difficult to think of types of light which would be expected to have super-Poissonian statistics. If there are any classical fluctuations in the intensity, then we would expect to observe larger photon number fluctuations than for the case with a constant intensity. Since a perfectly stable intensity gives Poissonian statistics, it follows that all classical light beams with time-varying light intensities will have super-Poissonian photon number distributions. Sub-Poissonian light, by contrast, has a narrower distribution than the Poissonian case and is therefore 'quieter' than perfectly coherent light.

Now we have already emphasized that a perfectly coherent beam is the most stable form of light that can be envisaged in classical optics. It is therefore apparent that sub-Poissonian light has no classical counterpart, and is therefore the first example of non-classical light that we have met. The table below gives a summary of the classification of light according to the criteria established in this section.

Sub-Poissonian light is defined by the relation:

$$\Delta n < \sqrt{\bar{n}}.$$

It is apparent from Figure 4 that sub-Poissonian light has a narrower photon number distribution than for Poissonian statistics. We have seen that a perfectly coherent beam with constant intensity has Poissonian photon statistics. We thus conclude that sub-Poissonian light is somehow more stable than perfectly coherent light, which has been our paradigm up to this point. In fact, sub-Poissonian light has no classical equivalent. Therefore, the observation of sub-Poissonian statistics is a clear signature of the quantum nature of light. Even though there is no direct classical counterpart of sub-Poissonian light, it is easy to conceive of conditions that would give rise to sub-Poissonian statistics. Let us consider the properties of a beam of light in which the time intervals Δt between the photons are identical, as illustrated schematically in Figure 5. The photocount obtained for such a beam in a time T would be the integer value determined by:

$$N = \mathrm{Int}\left(\eta \frac{T}{\Delta t}\right),$$

which would be exactly the same for every measurement.

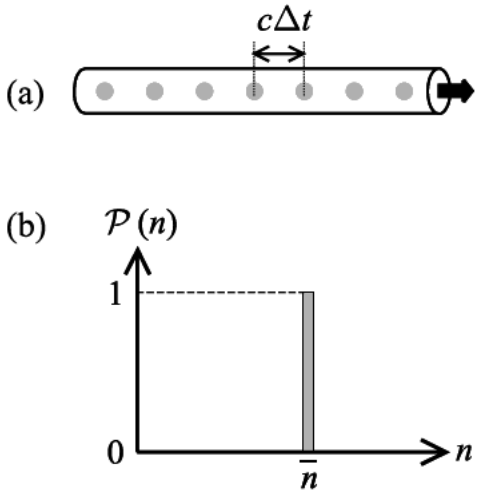

Figure 5. (a) A beam of light containing a stream of photons with a fixed time spacing Δt between them. (b) Photon-counting statistics for such a beam.

The experimenter would therefore obtain the histogram shown in Figure 5(b), with $\bar{n} = N$. This is highly sub-Poissonian, and has $\Delta n = 0$. Photon streams of the type shown in Figure 5(a) with $\Delta n = 0$ are called photon number states. Other types of sub-Poissonian light can be conceived in which the time intervals between the photons in the beam are not exactly the same, but are still more regular than the random time intervals appropriate to a beam with Poissonian statistics. Such types of light are fairly easy to generate in the laboratory, although their detection is quite problematic.

1.4 . Degradation of photon statistics by losses

Another important point one should consider during photon statistics is issue related to optical losses.

Let us suppose that we have a beam of light that passes through a lossy medium and is then detected as shown in Figure 6(a). If the transmission of the medium is T , then we can model the losses as a beam splitter with splitting ratio $T : (1 - T)$, as indicated in Figure 6(b). The beam splitter separates the photons into two streams going towards its two output ports, so that only a fraction T of the incoming photons impinge on the detector and are registered as counts. Now the beam splitting process occurs randomly at the level of individual photons, with weighted probabilities for the two output paths of $T : (1 - T)$, respectively. We therefore see that the lossy medium randomly selects photons from the incoming beam with probability T . It is well known that the distribution obtained by random sampling of a given set of data is more random than the original distribution. This point is illustrated in Figure 6(c), which presents the case of a regular stream of photons split with 50 : 50 probability towards two output ports. It is apparent that the regularity of the time intervals in the photon stream going to the detector is

reduced compared to the incoming photon stream. Thus the random sampling nature of optical losses degrades the regularity of the photon flux, and would eventually make the time intervals completely random for low values of *T*.

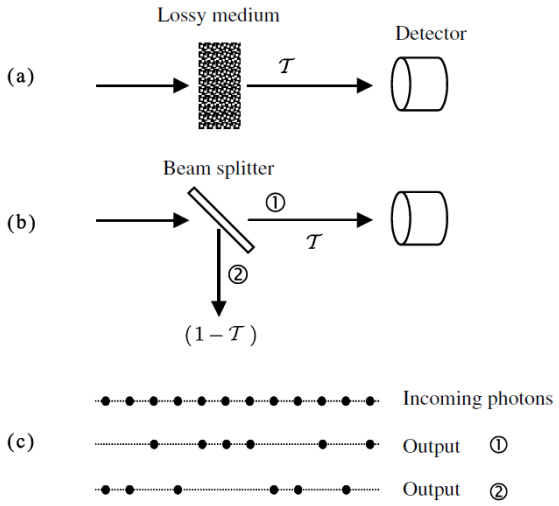

Figure 6. (a) The effect of a lossy medium with transmission T on a beam of light can be modelled as a beam splitter with splitting ratio $T : (1 - T)$ as shown in (b). The beam splitting process is probabilistic at the level of the individual photons, and so the incoming photon stream splits randomly towards the two outputs with a probability set by the transmission: reflection ratio (50: 50 in this case) as shown in part (c).

The beam splitter model of optical losses is a convenient way to consider the many different factors that reduce the efficiency of photon-counting experiments. These factors include:
(1) Inefficient collection optics, whereby only a fraction of the light emitted from the source is collected;
(2) Losses in the optical components due to absorption, scattering, or reflections from the surfaces;
(3) Inefficiency in the detection process due to using detectors with imperfect quantum efficiency
All of these processes are equivalent to random sampling of the photons. The first one randomly selects photons from the source. The second randomly deletes photons from the beam. The third randomly selects a subset of photons to be detected. The first two degrades the photon statistics themselves, while the third degrades the correlation between the photon statistics and the photoelectron statistics. Therefore, we must be very careful to avoid optical losses and use very high-efficiency detectors to observe large quantum effects in the photon statistics.

1.5. Theory of photodetection

Now that we are familiar with the different types of photon statistics that can occur, it is appropriate to consider the relationship between the counting statistics registered by the detector and the underlying photon statistics of the light beam.

Let us consider a photon-counting detector such as an avalanche photodiode or photomultiplier

illuminated by a faint light beam. The light interacts with the atoms in the detector and liberates individual electrons by the photoelectric effect. These single photoelectrons then trigger the release of many more electrons in the multiplier region of the tube (as in the case of photomutiplier), thereby generating a current pulse of sufficient magnitude to be detected with an electronic counter.

In this experiment a Single-Photon Avalanche Diode (SPAD) is used for the detection of photons. SPAD defines a class of photodetectors able to detect low intensity signals (down to the single photon) and to signal the time of the photon arrival with high temporal resolution (few tens of picoseconds). SPADs, like the Avalanche photodiode (APD), exploits the photon-triggered avalanche current of a reverse biased p-n junction to detect an incident radiation. The fundamental difference between SPADs and APDs is that SPADs are specifically designed to operate with a reverse bias voltage well above the breakdown voltage (on the contrary APDs operate at a bias lesser than the breakdown voltage). This kind of operation is also called Geiger-mode in literature, for the analogy with the Geiger counter.

SPADs are semiconductor devices based on a p-n junction reversed biased at a voltage higher than the breakdown voltage. At this bias, the electric field is so high that a single charge carrier injected in the depletion layer can trigger a self-sustaining avalanche. The current rises swiftly (sub nanosecond rise-time) to a macroscopic steady level, in the milliampere range. If the primary carrier is photo-generated, the leading edge of the avalanche pulse marks (with picosecond time jitter) the arrival time of the detected photon. The current continues to flow until the avalanche is quenched by lowering the bias voltage down: the lower electric field is no longer able to accelerate the carriers to impact-ionize with lattice atoms, therefore current ceases. In order to be able to detect another photon, the bias voltage must be raised again above breakdown. These operations require a suitable circuit, which has to i) sense the leading edge of the avalanche current; ii) generate a standard output pulse synchronous with the avalanche build-up; iii) quench the avalanche by lowering the bias down to the breakdown voltage; iv) restore the photodiode to the operative level. This circuit is usually referred to as a quenching circuit.

The SPADs that will be used in this experiment has specifications as shown in table 1.

Specifications @ 25°C and 5V overvoltage	Min	Typ	Max	Units
Photon Detection Efficiency @ 400nm @ 550nm @ 650nm	 21 45 34	 24 49 37		%
Single Photon Timing Resolution TTL Counting Output NIM Timing Output (additional internal circuit board required)		 35	 250 50	ps (FWHM)
After-pulsing probability	0.1		3	%
Dead Time		77		ns
Supply Voltage	unregulated DC, any value 5V ~ 12V			
TTL Output Pulse rise and fall times Output pulse duration Gating input Supply input connector	< 2ns on 10pF load 20ns typical 5V CMOS control (0V, detector off) Standard 3.5mm supply socket			

Table 1. Specifications of SPADs (Micro Photon Devices).

2. Second order correlation $g^{(2)}(\tau)$ and light sources

In the previous section we classified light beams according to their photon statistics. We saw that the observation of Poissonian and super-Poissonian statistics could be explained by classical wave theory, but not sub-Poissonian statistics. Hence sub-Poissonian statistics is a clear signature of the photon nature of light. In this section we will look at a different way of quantifying light according to the second-order correlation function $g^{(2)}(\tau)$. This will lead to an alternative threefold classification in which the light is described as *antibunched*, *coherent*, or *bunched*. We shall see that antibunched light is only possible in the photon interpretation, and is thus another clear signature of the quantum nature of light. These effects were first investigated in detail by R. Hanbury Brown and R. Q. Twiss (HBT) in the 1950s [2], and their work has subsequently proven to be of central importance in the development of modern quantum optics.

Figure 7(a) illustrates the experimental arrangement for a HBT experiment configured with single photon counting detectors. A stream of photons is incident on a 50 : 50 beam splitter, and is divided equally between the two output ports. The photons impinge on the detectors and the resulting output pulses are fed into an electronic counter/timer. The counter/timer records the time that elapses between the pulses from D1 and D2, while simultaneously counting the number of pulses at each input. The results of the experiment are typically presented as a histogram, as shown in Figure 7(b). The histogram displays the number of events that are registered at each value of the time τ between the start and stop pulses.

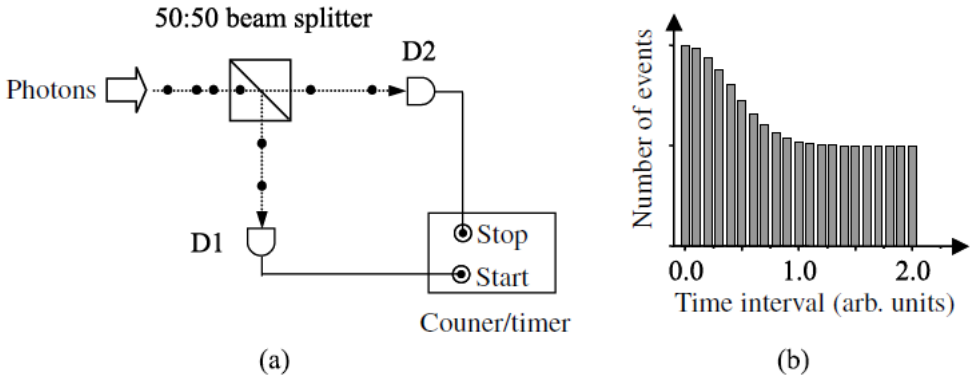

Figure 7. (a) Hanbury Brown–Twiss (HBT) experiment with a photon stream incident on the beam splitter. The pulses from the single-photon counting detectors D1 and D2 are fed into the start and stop inputs of an electronic counter/timer. The counter/timer both counts the number of pulses from each detector and also records the time that elapses between the pulses at the start and stop inputs. (b) Typical results of such an experiment. The results are presented as a histogram showing the number of events recorded within a particular time interval. In this case the histogram shows the results that would be obtained for a bunched photon stream.

Since the number of counts registered on a photoncounting detector is proportional to the intensity, one can write the second order correlation function of $g^{(2)}(\tau)$ as:

$$g^{(2)}(\tau) = \frac{\langle n_1(t) n_2(t+\tau) \rangle}{\langle n_1(t) \rangle \langle n_2(t+\tau) \rangle}, \qquad (1)$$

where $n_i(t)$ is the number of counts registered on detector i at time t. This shows that $g^{(2)}(\tau)$ is dependent on the simultaneous probability of counting photons at time t on D1 and at time $t + \tau$ on D2. In other words, $g^{(2)}(\tau)$ is proportional to the conditional probability of detecting a second photon at time $t = \tau$, given that we detected one at $t = 0$. This is exactly what the histogram from the HBT experiment with photoncounting detectors records. Hence the results of the HBT experiment also give a direct measure of the second-order correlation function $g^{(2)}(\tau)$ in the photon interpretation of light. Keep in mind that this is valid only when the multiphoton probability is low. One important property of $g^{(2)}(\tau)$ for a light source is that its value does not change with loss as long as all modes experience the same loss (e.g., transmission through a beam splitter does not change the second order coherence). To gain more insight into the multi-photon probability and further information contained in the second order correlation function for pulsed and CW sources, one can find a detail in reference [3].

Now let us suppose that the incoming light consists of a stream of photons with long time intervals between successive photons. The photons then impinge on the beam splitter one by one and are randomly directed to either D1 or D2 with equal probability. There is therefore a 50% probability that a given photon will be detected by D1 and trigger the timer to start recording. The generation of a start pulse in D1 implies that there is a zero probability of obtaining a stop pulse from D2 from this photon. Hence the timer will record no events at $\tau = 0$. Now consider the next photon that impinges on the beam splitter. This will go to D2 with

probability 50%, and if it does so, it will stop the timer and record an event. If the photon goes to D1, then nothing happens and we have to wait again until the next photon arrives to get a chance of having a stop pulse. The process continues until a stop pulse is eventually achieved. This might happen with the first or second or any subsequent photon, but never at τ =0. We therefore have a situation where we expect no events at τ =0, but some events for larger values of τ, which clearly contravenes the classical results. We thus immediately see that the experiment with photons can give results that are not possible in the classical theory of light. The observation of the non-classical result with $g^{(2)}(\tau) = 0$ arose from the fact that the photon stream consisted of individual photons with long time intervals between them. Let us now consider a different scenario in which the photons arrive in bunches. Half of the photons are split towards D1 and the other half towards D2. These two subdivided bunches strike the detectors at the same time and there will be a high probability that both detectors register simultaneously. There will therefore be a large number of events near τ =0. On the other hand, as τ increases, the probability for getting a stop pulse after a start pulse has been registered decreases, and so the number of events recorded drops. We thus have a situation with many events near τ =0 and fewer at later times, which is fully compatible with the classical results. In general there are threefold classification of light according to the second-order correlation function $g^{(2)}(\tau)$.

- bunched light: $g^2(0) > 1$,
- coherent light: $g^2(0) = 1$,
- antibunched light: $g^2(0) < 1$.

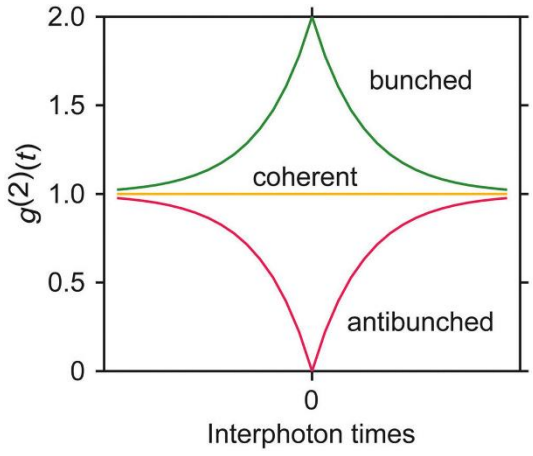

Figure 8. The second-order coherence function $g^{(2)}$ versus interphoton time for antibunched, coherent (laser), and bunched (thermal) light sources. $g^{(2)}(0)=0$ means that all the photons are separated in time.

Figure 9 is a simplistic attempt to illustrate the difference between the three different types of light in terms of the photons streams. The reference point is the case where the time intervals between the photons are random. On either side of this we have the case where the photons spread out with regular time intervals between them, or where they clump together in bunches. These three cases correspond to coherent, antibunched, and bunched light, respectively. In what follows below, we explore the properties of each of these three types of light in more detail, starting with coherent light.

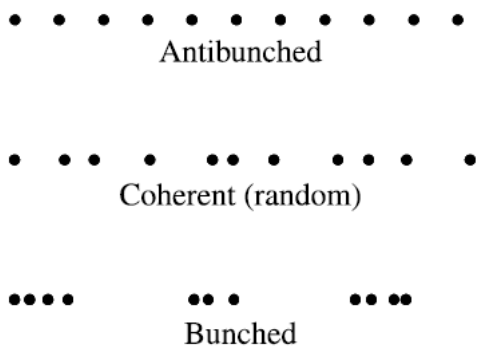

Figure 9. Comparison of the photon streams for antibunched light, coherent light, and bunched light. For the case of coherent light, the Poissonian photon statistics correspond to random time intervals between the photons.

2.1 *Photon antibunching measurements with continuous wave (CW) laser excitation*

A typical configuration to determine photon antibunching in a fluorescence signal, i.e., to measure the intensity autocorrelation function at short (ns) lag times, uses a regular confocal microscope scheme for excitation of the sample (see Figure 10). A CW-laser (532 nm wavelength, CPS 532 - Collimated Laser Diode Module, Thorlabs GmbH) is focused to a diffraction limited spot and the fluorescence from the sample is collected by the same objective as used for illumination. The laser light is separated from fluorescence photons by a dichroic mirror and further spectrally filtered using two long pass filters that have cut-on wavelength at 550 nm (FELH0550, Thorlabs GmbH) to suppress the scattered laser light. A confocal pinhole of 50 µm diameter selects the focal plane of the emitter and gets rid of the unwanted background signal. A flippable reflecting mirror that is placed along the optical axis of the setup sends the fluorescence signal to the imaging camera. Imaging helps to identify the quantum emitters and align them along the optical axis for detection as shown in Figure 11(a). The spectrometer (Flame-S-VIS-NIR-ES, Ocean Optics GmbH) is used to investigate the spectral feature of the emitters (Figure 11(b)). A 50/50 non-polarizing beam splitter sends the emitted photons to the two single-photon avalanche photodiodes (SPADs) (Micro Photon Devices, 100 µm active area, < 50 ps jitter and < 250 cps dark count). These detectors are connected to the start-stop time-interval analyzer of a time-correlated single photon counter (TCSPC) (TimeHarp 260 Nano, PicoQuant GmbH) and the delay between the arrival times of two emitted photons will be repeatedly measured and histogrammed with 250 picosecond time resolution to determine the photon statistics. Note that the technical note [4] gives a theoretical overview about Time-Correlated Single Photon Counting (TCSPC). It provides information about basic principles such as count rate statistics, timing resolution and the characteristics of photon counting detectors.

Figure 12 shows the complete experimental setup. The right side of Figure 12 depicts the HBT interferometer used in this experiment.

To experimentally determine the autocorrelation function, the fluorescence intensity should be explored over large time scales. One can rewrite the autocorrelation function (equation 1) in terms of fluorescence intensity I(t) and ensemble averaging <> as:

$$g^{(2)}(t, t+\tau) = \frac{\langle I(t)I(t+\tau)\rangle}{\langle I(t)\rangle\langle I(t+\tau)\rangle} \quad (2)$$

Both the time analyzer and the correlator give numbers of coincidence counts n(τ) as a function of the time delay between photons. The normalized autocorrelation function can be deduced by calculating $g^{(2)}(\tau) = n(\tau)/I_A I_B \Delta t T$, where I_A and I_B are the mean intensities on the start and stop channels, Δt the time resolution and T the total acquisition time.

The histogram of coincidence counts at short time scale shows a dip centered at τ= 0. The dip can be described by an exponential curve as:

$$g^{(2)}(\tau) = a(1 - be^{\tau/\tau_0}) \quad (3)$$

For an excitation intensity I well below the saturation limit, the value of τ_0 is essentially determined by the excited state lifetime.

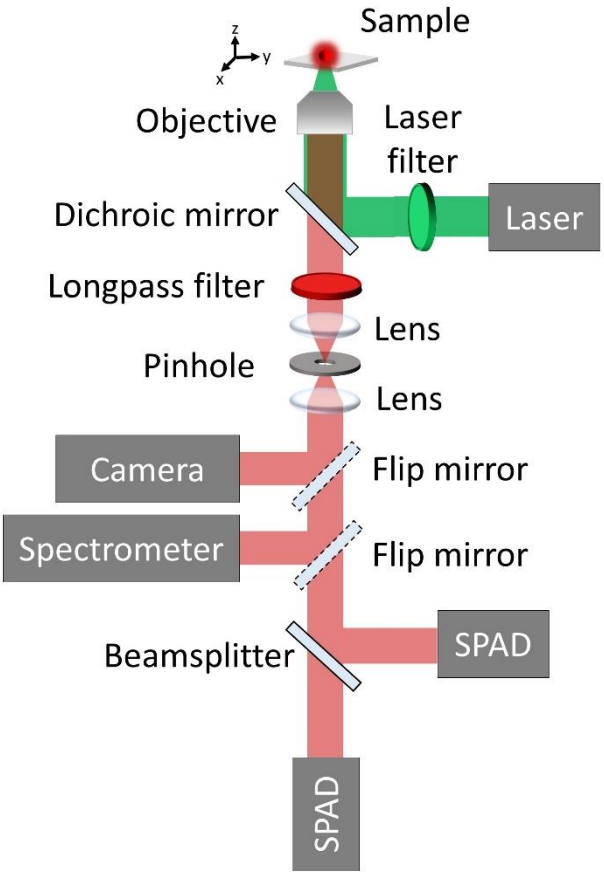

Figure 10. Schematic of the optical setup for measuring the photon statistics of different light sources.

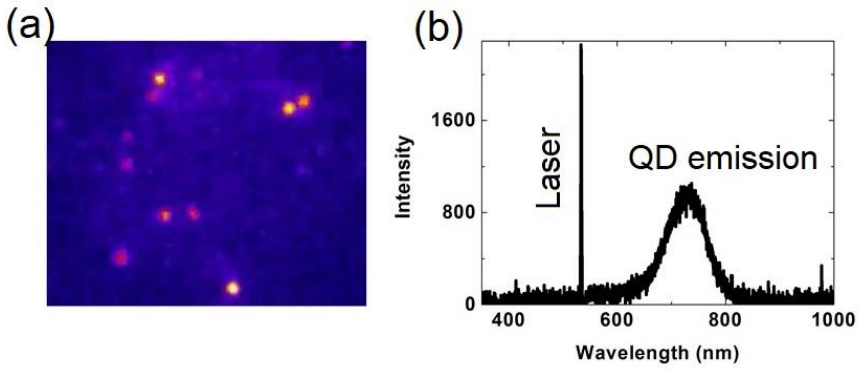

Figure 11. (a) Fluorescence image of QDs. (b) Emission spectrum of QDs excited with 532 nm laser.

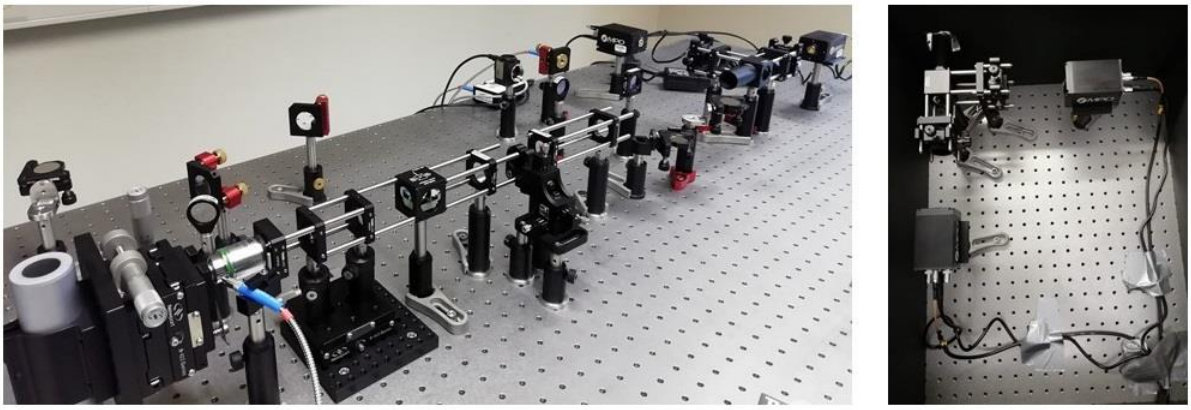

Figure 12. Experimental setup for measuring the second order correlation $g^{(2)}(\tau)$ of different light sources.

Antibunching has been observed from many types of light emitters, including a number of solid-state sources, such as:

• fluorescent dye molecules doped in a glass or crystal;
• semiconductor quantum dots;
• colour centres in diamonds.

In this experiment we will use semiconductor quantum dots as a single photon source. In the following their properties will be introduced.

2.2 Quantum dots as a single photon source

Quantum dots (QDs) are semiconductor nanoparticles that exhibit size dependent optical and electronic properties due to quantum confinement effects. In recent years they are a central topic in nanotechnology due to their applications as single-photon sources, solar cells, LEDs, Lasers, quantum computing and medical imaging.

When the quantum dots are illuminated by light, an electron in the quantum dot can be excited to a state of higher energy. That corresponds to the transition of an electron from the valance band to the conduction band. The excited electron drops back into the valence band by the releasing the energy in the form of light (photons). This light emission (the so called photoluminescence) is illustrated in Figure 13(a). The color (wavelength) of the emitted light

depends on the size of the QDs. This is due to size dependant bandgap modification of the nanocrystals. Larger QDs (more than 5 nm diameter) emit at longer wavelengths (e.g., colors such as orange or red). Smaller QDs of size between 2–5 nm usually emit shorter wavelengths (e.g., colors like blue and green) as shown in Figure 13(b). However, the specific colors vary depending on the exact composition of the QD. In this experiment we will use colloidally synthesized CdSe/ZnS QDs.

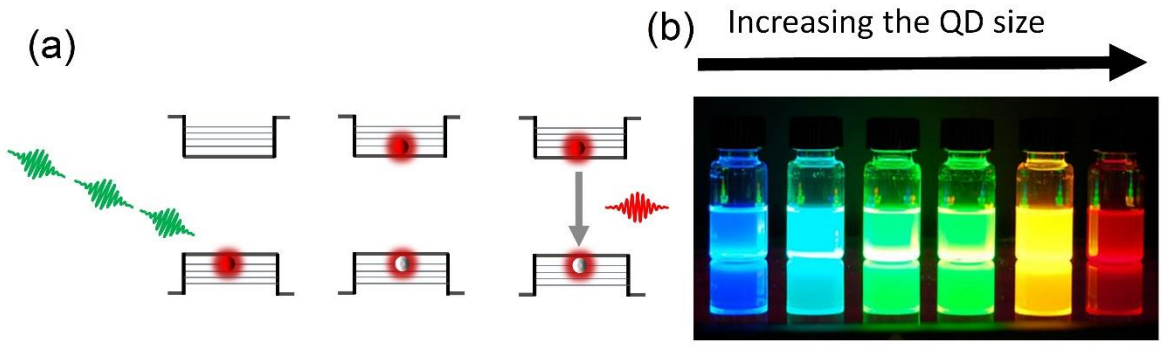

Figure 13. (a) Excitation of an electron by a laser light followed by fluorescence emission from a QD. (b) The color (wavelength) of the emitted light depends on the size of the QDs.

3. Experimental background and Procedures

In the following the experimental procedure for sample preparation and optical measurements will be presented.

3.1 Sample preparation*:* The CdSe/ZnS (core/shell) quantum dot is in a powder form and it is highly luminescent semiconductor nanocrystal coated with hydrophobic organic molecules. Therefore, it is readily soluble in heptane, toluene, chloroform but not soluble in water, alchols and ethers. The diameter of CdSe is 4.9 nm and its shell has 0.6 nm thickness. The QD solution can be prepared using one of the mentioned solvent and drop casted or spin coated on a cover slide. The distribution of the QDs on the cover slides should be made in such a way that one obtains one QD in 1 μm^2. Let us call this distribution as "single emitter distribution" and follow the following procedure for the preparation of your sample.

1. Use 0.5 mg of QDs powder to determine the concentration of QD solution you need for single emitter distribution. This can be done first by calculating the Molarity of the solution. Molarity is the most common term to describe the concentration of a solution. It is equal to the mole of solute divided by the liters of solution. The solute is defined as the substance being dissolved (QDs), while the solvent is the substance where the solute is dissolved (toluene). Remind that the number of moles of solute is equal to mass of solute divided by molar mass of solute. Before preparing the solution (putting the QDs in to the solvent) please show your calculations and discuss how much solvent you need to obtain single emitter distribution.
2. After the preparation of the solution, drop cast the QDs solution on a cover slip. Prepare 2 samples using this technique.
3. Use another 2 cover slip and spin coat the QDs solution. The parameters for spin coating will be provided by the supervisor.

Remind that sample preparation will be performed after you get training on how to work in the chemistry laboratory. Solution preparation, drop casting and spin coating techniques will also be introduced to you.

3.2 Optical measurements*:* Optical characterization of the sample (QDs on a cover slip) is performed using micro-photoluminescence setup as discussed in session 2.1. After putting the sample on the sample stage and determining the polarization of the laser and its power, follow the following procedures.

1. Using the neutral density filter decrease the laser power and excite the sample. Use the camera to identify the emitters and align precisely along the optical axis for detection.
2. Measure the fluorescence spectrum using the spectrometer.
3. Use the HBT interferometer configured with single photon counting detectors to record the number of events that are registered at each value of the time τ between the start and stop pulses.
4. Explain why the second order correlation function measurement for a single QD deviate from the ideal $g^{(2)}(0) = 0$ result. Use equation (3) to fit the measured second order correlation function.
5. Finally, chaotic and coherent light sources will be provided and determine their photon statistics and measure the second order correlation function. Compare the result with single QD measurement and discuss their difference.

4. Data Analysis and Report format

A good lab report does more than presenting data; it demonstrates the writer's comprehension of the concepts behind the data. Merely recording the expected and observed results is not sufficient; you should also identify how and why differences occurred, explain how they affected your experiment, and show your understanding of the principles the experiment was designed to examine. Bear in mind that a format, however helpful, cannot replace clear thinking and organized writing. You still need to organize your ideas carefully and express them coherently.

Typical components to be fulfilled are: Title Page, Abstract, Introduction, Methods and Materials (or Equipment), Experimental Procedure, Results, Discussion, Conclusion, References.

Prepared by: Dr. Assegid M. Flatae, Prof. Dr. Mario Agio and Philipp Reuschel

References

1. M. Fox, *Quantum Optics: An Introduction*, Oxford Master Series in Physics (2006).
2. R. Hanbury Brown, R. Q. Twiss, A Test of a New Type of Stellar Interferometer on Sirius, Nature, 178, 1046 (1956).
3. A. Migdall, S. V. Polyakov, J. Fan, J. C. Bienfang, *Single-Photon Generation and Detection*, Physics and Applications (Experimental Methods in the Physical Sciences), Volume 45 (2013).
4. M. Wahl, *Time-Correlated Single Photon Counting*, PicoQuant Technical Note (2014) (http://www.picoquant.com/images/uploads/page/files/7253/technote_tcspc.pdf).